ISA Transactions 90 (2019) 30–40

Contents lists available at ScienceDirect

ISA Transactions

journal homepage: www.elsevier.com/locate/isatrans

Research article

# An enhanced tracking control of marine surface vessels based on adaptive integral sliding mode control and disturbance observer

Mien Van

*The Institute of Research and Development, Duy Tan University, Viet Nam*

## HIGHLIGHTS

- A new composite integral sliding mode control and disturbance observer is developed.
- The backstepping control technique is designed as the nominal controller for integral sliding mode control.
- An integrating between disturbance observer and adaptive technique is developed to reduce chattering.
- The globally asymptotic stability of the system is guaranteed based on Lyapunov criterion.

## ARTICLE INFO

*Article history:*
Received 4 July 2018
Received in revised form 25 November 2018
Accepted 27 December 2018
Available online 25 January 2019

*Keywords:*
Integral sliding mode control
Adaptive control
Backstepping control technique
Disturbance observer
Surface vessels

## ABSTRACT

In this paper, a new control methodology is developed to enhance the tracking performance of fully actuated surface vessels based on an integrating between an adaptive integral sliding mode control (AISMC) and a disturbance observer (DO). First, an integral sliding mode control (ISMC), in which the backstepping control technique is used as the nominal controller, is designed for the system. The major features, i.e., benefits and drawbacks, of the ISMC are discussed thoroughly. Then, to enhance the tracking performance of the system, an adaptive technique and a new disturbance observer based on sliding mode technique are developed and integrated into the ISMC. The stability of the closed-loop system is proved based on Lyapunov criteria. Computer simulation is performed to illustrate the tracking performance of the proposed controller and compare with the existing controllers for the tracking control of a surface vessel. The simulation results demonstrate the superior performance of the proposed strategy.



## 1. Introduction

Marine Vessels have been providing important role for several major tasks in the sea such as transportation, ocean exploration, oil harvesting, etc., [1,2]. Since the vessels work in the extreme environment, the tracking control system faces huge challenge due to the presence of high model uncertainties and external disturbances [3,4]. Hence, in order to obtain the desired performance of the system, several advanced control methods have been developed. Firstly, linear controller has been employed for tracking control of the surface vessels. For example, in [5], a LQR controller has been developed for tracking control of the ships. Later, due to the inherent nonlinear characteristics of the surface vessels, nonlinear control methods have been developed. In [6] and [7,8], PD and PID controllers have been developed, respectively. In [9], backstepping control technique has been developed to stabilize the vessel based on Lyapunov criteria. Although the designs of PD, PID and conventional backstepping control technique are quite simple, they do not provide good robustness against the uncertainty and disturbance. Consequently, the performances of the systems are low. Due to their approximation capability, intelligent control techniques or learning techniques based on neural network (NN) [10–13] or fuzzy logic [14–17] have been developed. Recently, model predictive controls (MPCs) have also been developed to obtain optimal control input for the system [18–20]. The major disadvantage of the use of NN/fuzzy logic or MPC is that it requires high computational burden.

Since the vessels in the sea are always affected by the environmental disturbances, it is necessary to develop robust controller to suppress the effects of them. Sliding mode control (SMC), which is a well-known robust control technique, has shown to provide excellent tracking performance due to its robustness against the uncertainties and disturbances [21]. The SMCs have been extensively applied for the tracking control of surface vessels [22–24]. Due to the advantages of the backstepping control technique and the SMC, a hybrid controller named adaptive backstepping sliding mode control (adaptive BSMC) has also been developed [25]. Generally, the operation of the conventional SMC includes two stages. In the first stage, the system is forced to reach the sliding surface; this stage is usually called as reaching phase. Then, in the second stage, the system is kept to stay in the sliding surface

*E-mail address:* vanmien1@gmail.com.

https://doi.org/10.1016/j.isatra.2018.12.047
0019-0578/

in infinite time. It is unfortunate that the presence of the reaching phase could decrease the performance of the system, as has been pointed out in [26]. In order to circumvent this drawback, integral sliding mode control (ISMC) has been developed [26–30]. Compared to the conventional SMC, the ISMC would offer three major benefits [30]. First, the ISMC eliminates the reaching phase so that the system can guarantee the physical constraints from the starting position. Second, the ISMC eliminates the matched uncertainty and disturbance but does not amplify the magnitude of the unmatched disturbance. Third, the response of the system with the matched disturbance is identical to the response of the nominal system. Conceptually, the ISMC consists of two terms: a continuous nominal controller is used for controlling the nominal system (the system without the effects of the perturbation) and a discontinuous controller aims to robust against the effects of the perturbation. Due to the presence of the discontinuous function, the controller provides high-frequency chattering phenomenon. In order to reduce this undesired behavior, a popular method is to employ the boundary method [26,27].

On the other hand, to precisely estimate the effects of the uncertainties and disturbances acting on the surface vessels, a straightforward solution is to design uncertainty/disturbance observers. Working toward this direction, several observer-based control methods have been developed [31,32]. This technique has been employed for estimating disturbances of the ship [33]. A good review of the disturbance observers can be referred to [34]. In these control methods, disturbance observers (DOs) are firstly designed to approximate the uncertainty and disturbance components. Then, the estimated values are used to compensate the uncertainty and disturbance in the system using feedforward control technique. It should be noted that, to guarantee the existing condition of the SMC, the sliding gain needs to be larger than the bounded value of the uncertainty and disturbance in the system [21]. Unfortunately, the big sliding gain will generate big chattering. Therefore, a straightforward solution to reduce the chattering is to reduce the effects of the uncertainty and disturbance in the system. Based on this idea, DO has been employed into the SMC to compensate for the effects of the uncertainty and disturbance to reduce the chattering [35,36].

In this paper, a new composite adaptive ISMC and DO is developed to enhance the tracking performance of the surface vessels. According to the best of the author's knowledge, this is the first paper to develop ISMC integrating with DO for the surface vessels with rigorous stability analysis. First, the ISMC technique is developed for the surface vessel system, in which the nominal controller is designed based on the backstepping control technique to guarantee the stability of the nominal system. Then, an adaptive control law and a new nonlinear disturbance observer based on sliding mode are developed and integrated into the ISMC to reduce the chattering of the system. The stability of the closed-loop system is proved based on Lyapunov criteria. The computer simulation is used to illustrate the performance of the proposed controller for tracking control of the surface vessels. The simulation results verify that, when compared with other state-of-the-art controllers, the proposed method provides superior performance.

In summary, compared to the existing approaches, the main contributions of this paper can be summarized as follows:

- Compared to the existing controllers for the surface vessels such as conventional sliding mode control [22–24], the integral sliding mode control is proposed to get the three exciting properties mentioned above.
- Compared to the existing disturbance observer [31–33], a new disturbance observer based on sliding mode is proposed to get higher accuracy of the disturbance estimation.
- Compared to the conventional ISMC [26–30], a novel sliding surface based on the nominal dynamics model and the estimated disturbance is developed to reduce the chattering of the system.

**Table 1**
Notations of consistently unique parameters.

| Notation | Representative |
|---|---|
| $\eta, \upsilon$ | Position and velocity of the vessel, respectively |
| $u = \tau, u_0, u_s$ | Control input, nominal controller, switching controller |
| $u_d$ | Disturbance compensation term |
| $\Gamma(\eta, \upsilon)$ | Lumped nominal component |
| $\Delta(\eta, \upsilon, t)$ | Lumped model uncertainty |
| $x_d, \dot{x}_d, \ddot{x}_d$ | Desired position, velocity and acceleration trajectory, respectively |
| $\sigma$ | Integral sliding mode surface |
| $\rho$ | The bounded value of the lumped uncertainty |
| $\Omega$ | The bounded value of the derivative of the lumped uncertainty |
| $e, \dot{e}$ | Tracking error, derivative of tracking error |
| $\hat{\Delta}(\eta, \upsilon, t)$ | Estimated uncertainty |

The other parameters will be defined when it firstly appear.

The rest of this paper is organized as follows. Section 2 describes the problem formulation. The design of integral sliding mode control and composite adaptive integral sliding mode control and disturbance observer are presented in Sections 3 and 4, respectively. Section 5 verifies the performance of the system based on computer simulation. The conclusions are given in Section 6.

*Notations*: To get clearer about the formulations used in the next sections, the consistently unique parameters are briefly described as in Table 1.

## 2. Problem formulation

In this paper, the multiple-input-multiple-output (MIMO) dynamics of a 3 degree-of-freedom (3DOF) fully actuated marine surface vessel in the presence of model uncertainties and external disturbance is considered. The motion of the system can be described by two reference coordinate frames as illustrated in Fig. 1: (i) the earth-fixed frame denoted as $O_eX_eY_e$, and (ii) the body-fixed frame denoted as $O_bX_bY_b$. Based on the defined coordinate frames, the position of the vessel can be presented by the vector $\eta = \begin{bmatrix} x & y & \psi \end{bmatrix}^T \in \Re^3$, where $\begin{bmatrix} x & y \end{bmatrix}^T$ are the coordinate of the vessel's center of symmetry with reference to earth-fixed frame and $\psi$ represents the heading, which is the orientation angle with reference to the axis $O_eX_e$. The velocity of the vessel is denoted by $\upsilon = \begin{bmatrix} \upsilon_x & \upsilon_y & \upsilon_\psi \end{bmatrix}^T \in \Re^3$, where $\begin{bmatrix} \upsilon_x & \upsilon_y \end{bmatrix}^T$ are the surge and sway velocities and $\upsilon_\psi$ is the heave velocity. The kinematics model of the vessel, which relates the vessel's position vector to the vessel's velocity vector, can be expressed as:

$$\dot{\eta} = J(\psi)\,\upsilon \tag{1}$$

where $J(\psi)$ is the rotation matrix defined as $J(\psi) = \begin{bmatrix} \cos\psi & -\sin\psi & 0 \\ \sin\psi & \cos\psi & 0 \\ 0 & 0 & 1 \end{bmatrix}$, $J^{-1}(\psi) = J^T(\psi)$.

The dynamic model of the vessels, which describes the relationship between the vessel's velocity and the forces acting on the vessels, is described by [25,33]:

$$M\dot{\upsilon} + C(\upsilon)\upsilon + D(\upsilon)\upsilon + g(\eta) + f(\eta, \upsilon) = \tau + \tau_f \tag{2}$$

where $M \in \Re^{3\times3}$ is a symmetric positive definite inertia matrix, $C(\upsilon) \in \Re^{3\times3}$ is the Centripetal and Coriolis torques, and $D(\upsilon) \in \Re^{3\times3}$ is the damping matrix, $g(\eta)$ represents the gravitational forces. The vector $f(\eta, \upsilon) \in \Re^3$ denotes model uncertainties, $\tau \in \Re^3$ is the control input. $\tau_f \in \Re^3$ is the vector representing unknown and time-variant external environmental disturbances due to wind, waves and currents.

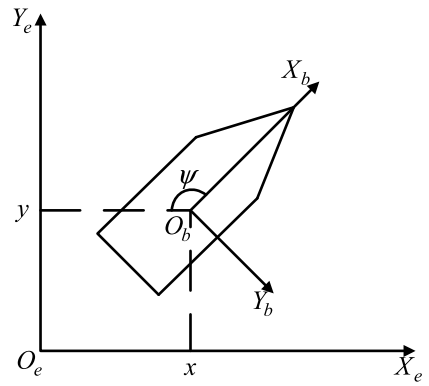


**Fig. 1.** Definition of reference coordinate frames of the vessel motion.

From (1) and (2), the composite dynamics model of the system can be rewritten as

$$\begin{aligned}\ddot{\eta} &= \dot{J}(\psi)\upsilon + J(\psi)\dot{\upsilon} \\ &= \dot{J}(\psi)\upsilon + J(\psi)M^{-1}\tau + J(\psi)M^{-1} \\ &\quad \left[\tau_f - C(\upsilon)\upsilon - D(\upsilon)\upsilon - g(\eta) - f(\eta,\upsilon)\right]\end{aligned} \tag{3}$$

Let $x_1 = \eta$, $x_2 = \dot{\eta}$, then the dynamics model of the surface vessel can be described as

$$\begin{aligned}\dot{x}_1 &= x_2 \\ \dot{x}_2 &= \dot{J}(\psi)\upsilon + J(\psi)M^{-1}\tau + J(\psi)M^{-1} \\ &\quad \left[\tau_f - C(\upsilon)\upsilon - D(\upsilon)\upsilon - g(\eta) - f(\eta,\upsilon)\right] \\ &= \Lambda\tau + \Lambda(-C(\upsilon)\upsilon - D(\upsilon)\upsilon - g(\eta)) \\ &\quad + \dot{J}(\psi)\upsilon + \Lambda\left(\tau_f - f(\eta,\upsilon)\right) \\ &= \Lambda u + \Gamma(\eta,\upsilon) + \Delta(\eta,\upsilon,t)\end{aligned} \tag{4}$$

where $u = \tau$, $\Lambda = J(\psi)M^{-1}$, $\Gamma(\eta,\upsilon) = \Lambda(-C(\upsilon)\upsilon - D(\upsilon)\upsilon - g(\eta)) + \dot{J}(\eta)\upsilon$ denotes the lumped nominal component and $\Delta(\eta,\upsilon,t) = \Lambda\left(\tau_f - f(\eta,\upsilon)\right)$ denotes the lumped uncertainty.

**Assumption 1.** The lumped uncertainty is bounded [33]:

$$\|\Delta(\eta,\upsilon,t)\| \le \rho \tag{5}$$

where $\rho$ is an unknown constant, and its derivative is satisfied:

$$\left\|\dot{\Delta}(\eta,\upsilon,t)\right\| \le \Omega \tag{6}$$

where $\Omega$ is a known constant.

In the practical engineering applications, the model uncertainty, i.e., $f(\eta,\upsilon)$, usually consists of structured and unstructured uncertainties. The structured uncertainty usually consists of the difference in nominal parameters of the dynamic matrices, i.e., $C(\upsilon)$, $D(\upsilon)$ and $g(\eta)$. Obviously, these values are bounded. The unstructured uncertainty is usually caused by the friction during rotating of the motors. The amount of the friction and the changing rates of the friction are usually bounded. In addition, since the environmental disturbance forces acting on the vessels are constantly changing and have finite energy, the disturbances acting on the vessel can be viewed as the time-varying yet bounded signals with the finite changing rates [33]. Therefore, the Assumption 1 is reasonable.

The objective of this paper is to design a control input $u$ such that the system can track the desired trajectory well despite the existing of the uncertainties and disturbance.

## 3. Design of integral sliding mode control for tracking control of surface vessels

In this section, the controller based on integral sliding mode control (ISMC) is described. The design of the ISMC is divided into three steps. First, the sliding surface is constructed. Then, the switching term is introduced. Finally, the nominal controller based on the backstepping control method is presented.

### 3.1. Design of integral sliding mode surface and switching term

The objective of this section is to design a controller based on the integral sliding mode control such that the system state, i.e., $x_1$, can track the desired trajectory, i.e., $x_d = \eta_d = \begin{bmatrix} x_d & y_d & \psi_d \end{bmatrix}^T$, precisely. To quantify the objective, the tracking errors denoted by $e$ and $\dot{e}$ are defined as $e = x_1 - x_d$ and $\dot{e} = x_2 - \dot{x}_d$.

To unify the tracking error $e$ and $\dot{e}$, the following filter error is reconstructed:

$$s = \dot{e} + Ke \tag{7}$$

where $K$ is a constant.

Differentiating (7) with respect to time and using (4), we have

$$\dot{s} = \ddot{e} + K\dot{e} = \Lambda u + \Gamma(\eta,\upsilon) + \Delta(\eta,\upsilon,t) - \ddot{x}_d + K\dot{e} \tag{8}$$

In Eq. (8), there are two high-order differential terms, i.e., $\ddot{x}_d$ ($x_d$ is assumed to be differentiable) and $\dot{e}$, which may generate noises in the system. The term $\ddot{x}_d$ is the desired acceleration of the trajectory, which can be computed offline, and no noise exists in this component. The only term that may generate noise is the component $\dot{e} = \dot{\eta} - \dot{\eta}_d$ due to the velocity measurement noise. To eliminate it, a low-pass filter is usually employed in the practical applications.

Based on the system (8), the integral sliding surface is selected as [27]

$$\sigma(t) = s(t) - s(0) - \int_0^t \left(\Lambda u_0 + \Gamma(\eta,\upsilon) - \ddot{x}_d + K\dot{e}\right) dt \tag{9}$$

where $s(0)$ defines the value of the sliding surface at the time $t = 0$. The term of $-s(0)$ is added to get the exciting property that $\sigma(0) = 0$. It means the reaching phase is eliminated. $u_0$ is the nominal controller, which will be designed later, to stabilize the nominal system (the system without the lumped uncertainty).

Differentiating the sliding surface (9) with respect to time, we have

$$\begin{aligned}\dot{\sigma} &= \left(\Lambda u + \Gamma(\eta,\upsilon) + \Delta(\eta,\upsilon,t) - \ddot{x}_d + K\dot{e}\right) \\ &\quad - \left(\Lambda u_0 + \Gamma(\eta,\upsilon) - \ddot{x}_d + K\dot{e}\right)\end{aligned} \tag{10}$$

The control input is proposed as

$$u = u_0 + u_s \tag{11}$$

where the switching term is selected as follows:

$$u_s = -\Lambda^{-1}(\rho + \varpi)sign(\sigma) \tag{12}$$

where $\varpi$ is a small positive constant and $\rho$ is selected as in Assumption 1.

Inserting the composite controller (11) and (12) into (10), we have

$$\dot{\sigma} = -(\rho + \varpi)sign(\sigma) + \Delta(\eta,\upsilon,t) \tag{13}$$

Define a Lyapunov function candidate $V = \frac{1}{2}\sigma^T\sigma$. Differentiating the Lyapunov function, we have

$$\begin{aligned}\dot{V} &= \sigma\dot{\sigma} \\ &= \sigma\left(-(\rho + \varpi)sign(\sigma) + \Delta(\eta,\upsilon,t)\right) \\ &= -(\rho + \varpi)|\sigma| + \Delta(\eta,\upsilon,t)\sigma \\ &< 0\end{aligned} \tag{14}$$

Therefore, based on the Lyapunov criterion, we can verify that the stability of the sliding surface is guaranteed.

### 3.2. Design of nominal controller based on backstepping control technique for the nominal system

From (4), the nominal system can be rewritten as

$$\begin{aligned}\dot{x}_1 &= x_2\\ \dot{x}_2 &= \Lambda u_0 + \Gamma(\eta, \upsilon)\end{aligned} \tag{15}$$

In order to guarantee the asymptotic stability of the nominal system, the following backstepping design procedure is developed for the system (15):

First the following common coordinate transformation is defined:

$$z_1(t) = x_1(t) - x_d(t) \tag{16}$$

$$z_2(t) = x_2(t) - \alpha_1(t) \tag{17}$$

where $\alpha_1(t)$ is the virtual controller to be designed later.

*Step 1* Differentiating (16) with respect to time and combining with the result in (17), we have

$$\begin{aligned}\dot{z}_1 &= \dot{x}_1(t) - \dot{x}_d(t)\\ &= z_2(t) + \alpha_1(t) - \dot{x}_d(t)\end{aligned} \tag{18}$$

The virtual controller (the virtual controller is selected such that when $z_2 = 0$, the system (18) becomes stable under the input of the virtual controller) is designed as:

$$\alpha_1(t) = -k_1 z_1(t) + \dot{x}_d(t) \tag{19}$$

where $k_1$ is a positive constant.

Adding the controller (19) into (18), we have

$$\dot{z}_1(t) = z_2(t) - k_1 z_1(t) \tag{20}$$

*Step 2*: Differentiating (17) with respect to time and combining with the second equation of (15) and the derivative of (19), we have:

$$\begin{aligned}\dot{z}_2(t) &= \dot{x}_2(t) - \dot{\alpha}_1(t)\\ &= \Lambda u_0 + \Gamma(\eta, \upsilon) + k_1 \dot{z}_1 - \ddot{x}_d\end{aligned} \tag{21}$$

The nominal controller is selected as

$$u_0 = \Lambda^{-1}\left(-\Gamma(\eta, \upsilon) + \ddot{x}_d - k_1 \dot{z}_1 - z_1 - k_2 z_2\right) \tag{22}$$

where $k_2$ is a positive constant.

Inserting the controller (22) into (21), we have:

$$\dot{z}_2(t) = -z_1 - k_2 z_2 \tag{23}$$

*Step 3*: In this step, a Lyapunov function candidate is defined as below:

$$V(z_1, z_2) = \frac{1}{2} z_1^2 + \frac{1}{2} z_2^2 \tag{24}$$

Differentiating the Lyapunov function with respect to time, one yields

$$\begin{aligned}\dot{V}(z_1, z_2) &= z_1 \dot{z}_1 + z_2 \dot{z}_2\\ &= z_1 (z_2 + \alpha_1 - \dot{x}_d) + z_2 \dot{z}_2\\ &= z_1 z_2 - k_1 z_1^2 + z_2 (-z_1 - k_2 z_2)\\ &= -k_1 z_1^2 - k_2 z_2^2\\ &\leq 0\end{aligned} \tag{25}$$

It can be seen that the system (15) with the transformed coordinate (16)–(17), the Lyapunov function defined in (24) and the computed derivative of the Lyapunov function in (25) satisfy the conditions (i), (ii) and (iii) of the Lyapunov stability criteria, which is described as in Appendix A. In fact, from (25), it is obtained that $\dot{V}(z_1, z_2) < 0$ everywhere except on the line $z_1 = z_2 = 0$ where $\dot{V}(z_1, z_2) = 0$. Furthermore, note that from (20) and (23) to provide $\dot{V}(z_1, z_2) = 0$, the system trajectory must evolve on $z_1 = z_2 = 0$. Hence, by applying LaSalle invariance principle [37], we can conclude that tracking errors $z_1$ and $z_2$ converge to zero and the closed-loop system is globally asymptotically stable.

**Remark 1.** Beside the backstepping control technique, other control methods such as PID, computed torque control (CTC), optimal control, etc., can be employed to design the nominal controller. This paper selects the backstepping control technique since it is simple in design and the stability of the system is guaranteed based on Lyapunov criteria.

## 4. Tracking control of surface vessels using adaptive integral sliding mode control and disturbance observer

In the previous section, the ISMC was introduced for the surface vessels. However, according to (12), the sliding gain was chosen based on the bounded value of the uncertainty and disturbance. This big sliding gain value provides big chattering in the system. In this section, to reduce the chattering, a new disturbance observer and an adaptive technique are developed and integrated into the ISMC.

### 4.1. Design of disturbance observer

The system (8) can be rewritten as

$$\dot{s} = \Psi(u, \eta, \upsilon, \ddot{x}_d, \dot{e}) + \Delta(\eta, \upsilon, t) \tag{26}$$

where $\Psi(u, \eta, \upsilon, \ddot{x}_d, \dot{e}) = \Lambda u + \Gamma(\eta, \upsilon) - \ddot{x}_d + K\dot{e}$.

The following observer is considered:

$$\dot{\hat{s}} = \Psi(u, \eta, \upsilon, \ddot{x}_d, \dot{e}) + \hat{\Delta}(\eta, \upsilon, t) \tag{27}$$

where $\hat{\Delta}(\eta, \upsilon, t)$ is the estimation of $\Delta(\eta, \upsilon, t)$.

Let $\theta = s - \hat{s}$. From (26) and (27), the following error is obtained:

$$\dot{\theta} = -\widetilde{\Delta}(\eta, \upsilon, t) \tag{28}$$

where,

$$\widetilde{\Delta}(\eta, \upsilon, t) = \hat{\Delta}(\eta, \upsilon, t) - \Delta(\eta, \upsilon, t) \tag{29}$$

Since $\dot{\theta}$ is not available, we use the first-order sliding mode differentiator [38] to obtain its estimation:

$$\begin{aligned}\dot{\lambda}_0 &= \lambda_1,\\ \lambda_1 &= -\xi_1 |\lambda_0 - \theta|^{1/2} sign(\lambda_0 - \theta) + \nu_1\\ \dot{\nu}_1 &= -\xi_2 sign(\nu_1 - \lambda_1)\end{aligned} \tag{30}$$

Using suitably chosen parameter of $\xi_i (i = 1, 2)$, we can achieve

$$\lambda_0 = \theta, \lambda_1 = \dot{\theta} \tag{31}$$

Therefore, from (27), (30) and (31), we have $\lambda_1 \cong -\widetilde{\Delta}(\eta, \upsilon, t)$.

The following auxiliary function is introduced to design the disturbance observer:

$$e_\phi = \Delta(\eta, \upsilon, t) - \varphi(s) \tag{32}$$

where $\varphi(s)$ is a function vector. For the sake of implementation, $\varphi(s)$ is chosen as a linear function with respect to $s$.

Differentiating (32) with respect to time and combining with the result in (26), we have:

$$\dot{e}_\phi = \dot{\Delta}(\eta, \upsilon, t) - \delta(s)\left(\Psi(u, \eta, \upsilon, \ddot{x}_d, \dot{e}) + \Delta(\eta, \upsilon, t)\right) \tag{33}$$

where $\delta(s) = (\partial\varphi(s)/\partial s)$ is a constant parameter. The estimation $\hat{\dot{e}}_\phi$ of $\dot{e}_\phi$ is introduced as follows:

$$\hat{\dot{e}}_\phi = -\delta(s)\left(\Psi(u, \eta, \upsilon, \ddot{x}_d, \dot{e}) + \hat{\Delta}(\eta, \upsilon, t)\right) \tag{34}$$

Next, the disturbance estimation is designed as:

$$\hat{\Delta}(\eta, \upsilon, t) = \hat{e}_\phi + \varphi(s) + \int Msign(\lambda_1) \tag{35}$$

where $\hat{e}_\phi$ is obtained from (34), $\varphi(s)$ was defined above, $\lambda_1$ is taken from (30) and $M$ is the sliding gain, which is selected such that $M > \Omega$.

The stability of the disturbance observer is stated as the following Theorem 1.

**Theorem 1.** *Suppose that the Assumption 1 is satisfied. Then, the disturbance estimate, i.e., $\hat{\Delta}$, of the disturbance observer can asymptotically estimate the real disturbance, i.e., $\Delta$, if the observer gain $\delta(s)$ is chosen such that $\dot{\tilde{\Delta}} = -\delta(s)\tilde{\Delta}$ is stable.*

**Proof.** Differentiating (35) with respect to time, we have

$$\begin{aligned} \dot{\hat{\Delta}}(\eta, \upsilon, t) &= \dot{\hat{e}}_\phi + (\partial\varphi(s)/\partial s)\,\dot{s} + Msign(\lambda_1) \\ &\approx \dot{\hat{e}}_\phi + (\partial\varphi(s)/\partial s)\,\dot{s} - Msign(\tilde{\Delta}) \end{aligned} \tag{36}$$

Adding (26) and (34) into (36), we have

$$\begin{aligned} \dot{\hat{\Delta}}(\eta, \upsilon, t) &= -\delta(s)\left(\Psi(u, \eta, \upsilon, \ddot{x}_d, \dot{e}) + \hat{\Delta}(\eta, \upsilon, t)\right) \\ &\quad +\delta(s)\left(\Psi(u, \eta, \upsilon, \ddot{x}_d, \dot{e}) + \Delta(\eta, \upsilon, t)\right) - Msign(\tilde{\Delta}) \\ &= -\delta(s)\left(\hat{\Delta}(\eta, \upsilon, t) - \Delta(\eta, \upsilon, t)\right) - Msign(\tilde{\Delta}) \end{aligned} \tag{37}$$

The time derivative of (29) along (37) is

$$\dot{\tilde{\Delta}} = -\delta(s)\tilde{\Delta} - Msign(\tilde{\Delta}) - \dot{\Delta}(\eta, \upsilon, t) \tag{38}$$

Define the Lyapunov function candidate $V = \frac{1}{2}\tilde{\Delta}^2$. Differentiating the Lyapunov function and combining with the results in (38), we have

$$\begin{aligned} V &= \tilde{\Delta}\dot{\tilde{\Delta}} \\ &= \tilde{\Delta}\left(-\delta(s)\tilde{\Delta} - Msign(\tilde{\Delta}) - \dot{\Delta}(\eta, \upsilon, t)\right) \\ &= -\delta(s)\tilde{\Delta}^2 - M\left|\tilde{\Delta}\right| - \tilde{\Delta}\dot{\Delta}(\eta, \upsilon, t) \\ &\le -\delta(s)\tilde{\Delta}^2 - M\left|\tilde{\Delta}\right| - \tilde{\Delta}\Omega \\ &\le -\delta(s)\tilde{\Delta}^2 \end{aligned} \tag{39}$$

Then, if Assumption 1 is satisfied and the observer gain $\delta(s)$ is chosen such that $\dot{\tilde{\Delta}} = -\delta(s)\tilde{\Delta}$ is stable, the Theorem 1 is guaranteed. This completes the proof.

**Remark 2.** According to [32–34], the conventional disturbance observer has a form below:

$$\hat{\Delta}(\eta, \upsilon, t) = \hat{e}_\phi + \varphi(s) \tag{40}$$

And, thus, the estimation error can be expressed as [32–34]:

$$\dot{\tilde{\Delta}} = -\delta(s)\tilde{\Delta} - \dot{\Delta}(\eta, \upsilon, t) \tag{41}$$

From (41), we can see that the estimation error converges to zero when the derivative of the disturbance, i.e., $\dot{\Delta}(\eta, \upsilon, t)$, converges to zero. Therefore, the conventional disturbance observer was designed based on the assumption that the derivative of the disturbance converges to zero in infinite time. In contrast, in the proposed method, from (38) and (39), we can see that the effects of the component $\dot{\Delta}(\eta, \upsilon, t)$ can be compensated by the term $Msign(\tilde{\Delta})$. Consequently, the estimation error can be converged in finite time, and therefore, the estimation accuracy is improved.

**Remark 3.** The additional sliding gain, i.e., $M$, was selected based on the bounded value $\Omega$ stated in condition (6) of the Assumption 1. However, even when the bounded value $\Omega$ is unknown, if the value of $M$ is chosen as big enough, the stability of the system can still be guaranteed. Literally, there are two cases that may occur when the bounded value, i.e., $\Omega$, is unknown. In the first case, if the value of $M$ is bigger than the real bounded value, i.e., $\Omega$, the stability of the system can be stated as in Theorem 1. In contrast, in the second case, if the value of $M$ is smaller than the value of $\Omega$, the stability of the system can still be guaranteed as similar analysis as for the conventional disturbance observer [32,33]. Nonetheless, the existing of the sliding mode component in the design of observer in (35) helps to get higher estimation accuracy than the conventional disturbance observer. Therefore, the value of $\Omega$ is not strictly required to be known in this paper.

### 4.2. Design of tracking control of surface vessels using adaptive integral sliding mode control and disturbance observer

In the developed controller (12), the sliding gain of the switching term is chosen to be bigger than the bounded value of the lumped uncertainty, i.e., $(\rho + \varpi)$. Thus, if the bounded value is big, the system needs to choose the big switching gain, which will provide big chattering. In order to reduce the chattering, the disturbance observer is integrated into the design of the ISMC. Based on the output of the disturbance observer, the uncertainty component can be expressed according to its estimation, as below:

$$\Delta(\eta, \upsilon, t) = \hat{\Delta}(\eta, \upsilon, t) + \zeta \tag{42}$$

where $\zeta$ is the disturbance approximation error. This error is assumed to be bounded by:

$$\|\zeta\| \le \kappa \tag{43}$$

where $\kappa$ is an unknown constant. Based on the analysis in [30], this assumption is reasonable for practical engineering applications.

Then, for the system (8), the controller can be modified as

$$u = u_0 + u_d + u_s \tag{44}$$

where $u_d$ is used to compensate for the effects of the disturbance in the system and it is designed as:

$$u_d = -\Lambda^{-1}\hat{\Delta}(\eta, \upsilon, t) \tag{45}$$

and the switching term $u_s$ is now designed as follows:

$$u_s = -\Lambda^{-1}(\hat{\kappa} + \varpi)sign(\sigma) \tag{46}$$

where $\hat{\kappa}$ is the approximation value of the bounded value $\kappa$, and it is selected as:

$$\dot{\hat{\kappa}} = \frac{1}{\gamma}|\sigma| \tag{47}$$

where $\gamma$ denotes the adaptation gain.

Consider a Lyapunov function candidate:

$$V = \frac{1}{2}\sigma^T\sigma + \frac{1}{2}\gamma\tilde{\kappa}^T\tilde{\kappa} \tag{48}$$

where $\tilde{\kappa} = \hat{\kappa} - \kappa$ is the adaptation error.

Differentiating the above Lyapunov function, we have

$$\begin{aligned} \dot{V} &= \sigma\dot{\sigma} + \gamma\tilde{\kappa}\dot{\tilde{\kappa}} \\ &= \sigma\begin{pmatrix}(\Lambda u + \Gamma(\eta, \upsilon) + \Delta(\eta, \upsilon, t) - \ddot{x}_d + K\dot{e}) \\ -(\Lambda u_0 + \Gamma(\eta, \upsilon) - \ddot{x}_d + K\dot{e})\end{pmatrix} + \gamma\left(\hat{\kappa} - \kappa\right)\dot{\hat{\kappa}} \end{aligned} \tag{49}$$

Adding the composite controller (44)–(47) into (49), we obtain

$$\begin{aligned} \dot{V} &= \sigma\dot{\sigma} + \gamma\tilde{\kappa}\dot{\tilde{\kappa}} \\ &= \sigma\left(\Lambda u_s + \zeta\right) + \gamma\left(\hat{\kappa} - \kappa\right)\dot{\hat{\kappa}} \\ &= \sigma\left(-(\hat{\kappa} + \varpi)sign(\sigma) + \zeta\right) + \left(\hat{\kappa} - \kappa\right)|\sigma| \\ &\le -\varpi|\sigma| \end{aligned} \tag{50}$$

Because $\varpi > 0$, $\dot{V}$ becomes negative semi-definite, i.e., $\dot{V} \leq -\varpi |\sigma|$. Using the Lyapunov criterion as described in Appendix A, the convergence of $\sigma$ and $\widetilde{\kappa}$ to zero are guaranteed.

**Remark 4.** The main drawback of the use of SMC in the practical applications is the chattering phenomenon. In the literature, several methods have been developed to reduce the chattering, such as boundary layer method [21], disturbance observer [35], or higher-order sliding mode (HOSM) [39,40]. In this paper, a new disturbance observer has been developed to reduce the chattering as described in Section 4. Although the chattering could be reduced by the disturbance observer, however, due to the presence of the discontinuous *sign* function in the proposed controller (46), the chattering is still present. To further reduce the chattering due to the presence of the *sign* function, the boundary method is employed. Therefore, the controller in (46) can be replaced by:

$$u_s = -\Lambda^{-1}(\hat{\kappa} + \varpi)\frac{\sigma}{|\sigma| + c} \tag{51}$$

where $c$ is a small positive constant. The selection of the parameter $c$ decides the trade-off between maintaining ideal performance and ensuring smooth control effort.

**Remark 5.** From (47) ($\dot{\hat{\kappa}} = \frac{1}{\gamma}|\sigma|$), the adaptation gain $\hat{\kappa}$ keeps increasing until the sliding surface $\sigma$ equals to zero; this symptom is called 'parameter drift problem'. Unfortunately, it is very difficult to achieve $\sigma = 0$, and thus, the drift problem is always occurred. To prevent the parameter drift problem, the following deadzone method is used:

$$\dot{\hat{\kappa}} = \begin{cases} 0 & if\ |\sigma| \leq \varepsilon \\ \dfrac{1}{\gamma}|\sigma| & if\ |\sigma| > \varepsilon \end{cases} \tag{52}$$

where $\varepsilon$ is the deadzone size. From (52), we can see that when the sliding surface is smaller than the deadzone size $\varepsilon$, the adaptation gain $\hat{\kappa}$ will stop increasing.

## 5. Results and discussions

In order to demonstrate the performance of the proposed controller, the simulation model is built based on Matlab/Simulink environment. In this simulation, the dynamics model of the surface vessel is expressed as in (1) and (2), where the parameters are selected as follows [25]:

$$M = \begin{bmatrix} 25.8000 & 0 & 0 \\ 0 & 24.6612 & 1.0948 \\ 0 & 1.0948 & 2.7600 \end{bmatrix} \tag{53}$$

$$C(\upsilon) = \begin{bmatrix} 0 & 0 & -24.6612\upsilon_y \\ 0 & 0 & 25.8\upsilon_x \\ 24.6612\upsilon_y + 1.0948\upsilon_\psi & -25.8\upsilon_x & 0 \end{bmatrix} \tag{54}$$

$$g(\eta) = \begin{bmatrix} 0 & 0 & 0 \end{bmatrix}^T \tag{55}$$

$$D(\upsilon) = \begin{bmatrix} D_1 & D_2 & D_3 \end{bmatrix} \tag{56}$$

where:

$$D_1(\upsilon) = \begin{bmatrix} 0.7225 + 1.3274|\upsilon_x| + 5.8664\upsilon_x^2 \\ 0 \\ 0 \end{bmatrix},$$

$$D_2(\upsilon) = \begin{bmatrix} 0 \\ 0.8612 + 36.2823|\upsilon_y| + 8.05|\upsilon_\psi| \\ -0.1025 - 5.0437|\upsilon_y| - 0.13|\upsilon_\psi| \end{bmatrix},$$

**Table 2**
Selected parameters of the controllers.

| Controller | Parameters | Value |
|---|---|---|
| Backstepping control | $\gamma_1, \gamma_2$ | 10, 10 |
| SMC | $\rho, \varpi, c$ | 100, 1, 0.1 |
| Adaptive BSMC [25] | Can be referred to [25] for parameters selection. | |
| ISMC | $\gamma_1, \gamma_2$ | 10, 10 |
| | $\rho, \varpi, c$ | 100, 1, 0.1 |
| AISMC+DO | The parameters of ISMC term are selected as the same the ISMC controller. | |
| | Adaptive gain $\gamma$ in (47) | 1 |
| | $\varepsilon$ in (52) | 0.01 |
| | Disturbance observer gain $\delta(s), M, \xi_1, \xi_2$ | diag(5,5,5), 20, 22, 30 |

$$D_3(\upsilon) = \begin{bmatrix} 0 \\ 0.845|\upsilon_y| + 3.45|\upsilon_\psi| - 0.1079 \\ 0.845|\upsilon_y| + 3.45|\upsilon_\psi| - 0.1079 \end{bmatrix}.$$

The assumed disturbance is:

$$d = \begin{bmatrix} 10.3 + 50\sin(0.5t) + 50\sin(0.1t) \\ -20.9 + 2\sin(0.5t - \pi/6) + 50\sin(0.3t) \\ -30\sin(0.9t + pi/3) - 30\sin(0.1t) \end{bmatrix} \tag{57}$$

The desired trajectory used in this paper is

$$\eta_d = \begin{bmatrix} x_d \\ y_d \\ \psi_d \end{bmatrix} = \begin{bmatrix} 4\sin(0.02t) \\ 2.5(1 - \cos(0.02t)) \\ 0.02t \end{bmatrix} \tag{58}$$

The initial states of the vessels are modeled as $\eta(0) = \begin{bmatrix} 1.2\,(\mathrm{m}) & 1.2\,(\mathrm{m}) & \pi/3\,(\mathrm{rad}) \end{bmatrix}$ and $\upsilon(0) = \begin{bmatrix} 0\,(\mathrm{m/s}) & 0\,(\mathrm{m/s}) & 0\,(\mathrm{rad/s}) \end{bmatrix}$.

In order to verify the performance of the developed control strategy, we compare the performance of five state-of-the-art controllers: conventional backstepping control (CBC), conventional sliding mode control (SMC), adaptive backstepping sliding mode control (adaptive BSMC), which has been proposed recently in [25], the proposed integral sliding mode control (ISMC) presented in Section 3 and the proposed adaptive integral sliding mode control and disturbance observer (AISMC+DO) presented in Section 4. The design of the CBC can be designed as in Section 3.2, the design of the SMC is presented in Appendix B, while the design of the Adaptive BSMC can be referred to [25]. The selected parameters of the controllers are shown in Table 2. Employing the controllers into the simulated surface vessel, the performances of the controllers are shown in Figs. 2–5. Particularly, Fig. 2 shows the tracking performance of the controllers in the $x$ and $y$ axes. From Fig. 2, we can see that the conventional SMC provides low oscillatory. However, it provides very slow convergence speed. In contrast, the CBC obtains higher convergence speed, but provides big oscillatory from the beginning position. On the other hand, generally, the Adaptive BSMC provides higher convergence speed compared to the backstepping control and the SMC. The oscillations from the beginning of the Adaptive BSMC is higher than the SMC but less than the backstepping control. This is because the Adaptive BSMC combined the advantages of the backstepping control and the SMC. In addition, the results in Fig. 2 also verify that the ISMC and the AISMC+DO provide higher transient response and convergence speed than the Adaptive BSMC, the SMC and the CBC. This means that the ISMC provides higher performance in terms of transient response and convergence speed than the conventional SMC. Figs. 3–5 show the tracking errors of the system in the $x$-axis, $y$-axis and $\psi$-axis, respectively. For the sake of comparison between the performance of the controllers, the root-mean-square-error (RMSE) of

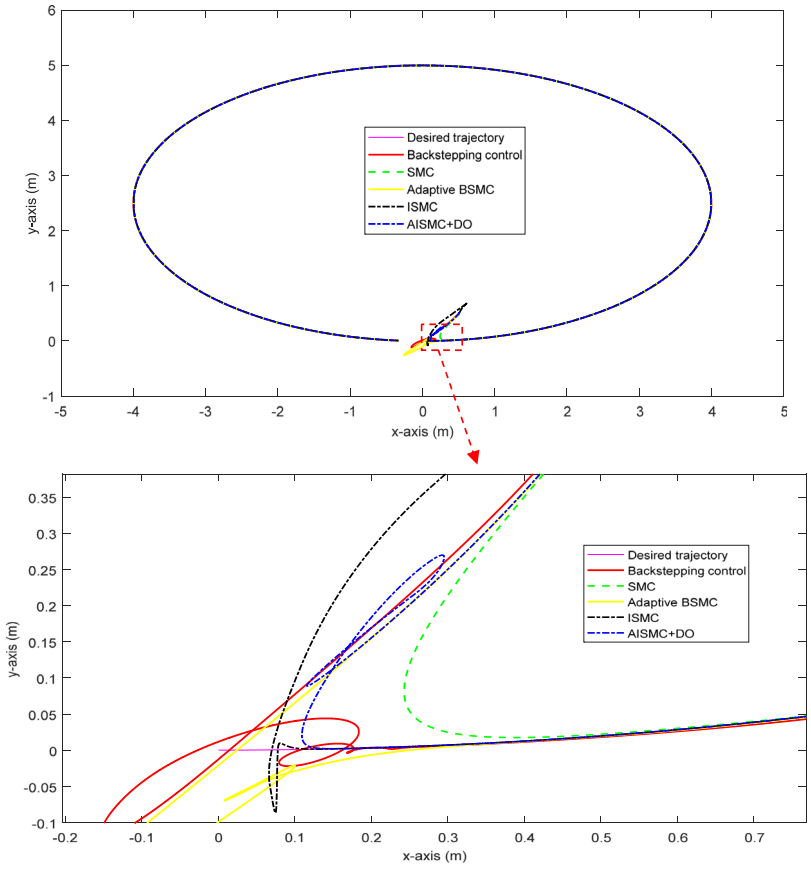


**Fig. 2.** Desired position trajectory and real position trajectory of the system under the Backstepping control, SMC, Adaptive BSMC, ISMC, and AISMC+DO.

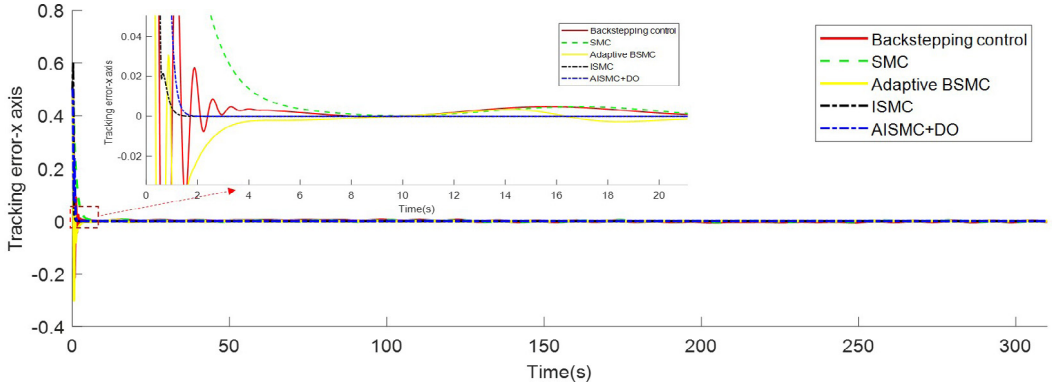


**Fig. 3.** Comparison in tracking error in $x$-axis among the Backstepping control, SMC, Adaptive BSMC, ISMC, and AISMC+DO.

the tracking errors of the system under these control methods are also reported in Table 3, where:

$$\|E_{xy}\| = \frac{1}{N}\sum_{i=1}^{N}\sqrt{\left(\|e_x(k)\|^2 + \|e_y(k)\|^2\right)} \tag{59}$$

$$\|E_{\psi}\| = \frac{1}{N}\sum_{i=1}^{N}\sqrt{\left(\|e_{\psi}(k)\|^2\right)} \tag{60}$$

where $N$ is the number of simulation steps.

From the results shown in Figs. 3–5, we can see that the oscillations of the CBC and the Adaptive BSMC are very big. The SMC provides small overshoot, but the convergence speed is very slow. The proposed methods, i.e., ISMC and ISMC+DO, obtain much better transient responses. As clearly shown in Fig. 5, the steady-state errors of the SMC, the CBC and the Adaptive BSMC are much bigger than the proposed methods, i.e., ISMC and ISMC+DO. The detail tracking errors of the controllers are reported in Table 3. From Table 3, we can see that the CBC and the SMC provide quite big tracking error. For instance, for $(xy)$-axis and $\psi$-axis, the backstepping control provides tracking errors of 0.0067 and 0.0136, respectively, as shown in Table 3. In contrast, for those axes, the tracking errors of the SMC are 0.0050 and 0.0147, respectively. By combining the advantages of the backstepping control and the SMC, the Adaptive BSMC provides lower tracking errors compared to the CBC and the SMC, and those are 0.0020 and 0.0021 for $(xy)$-axis and $\psi$-axis, respectively. Using the ISMC approach, the system gets lower tracking errors than the CBC, the SMC and the Adaptive BSMC. Particularly, the ISMC provides 0.0013 and $2.3915 \times 10^{-4}$

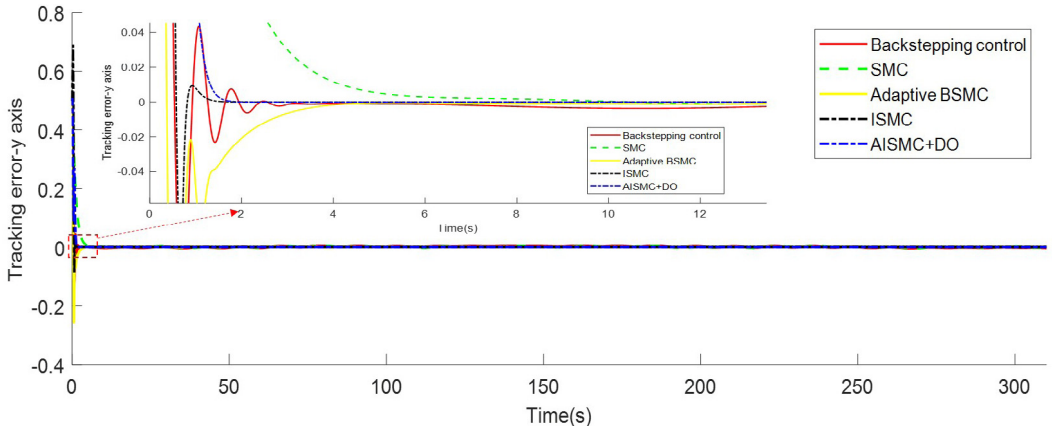


**Fig. 4.** Comparison in tracking error in $y$-axis among the Backstepping control, SMC, Adaptive BSMC, ISMC, and AISMC+DO.

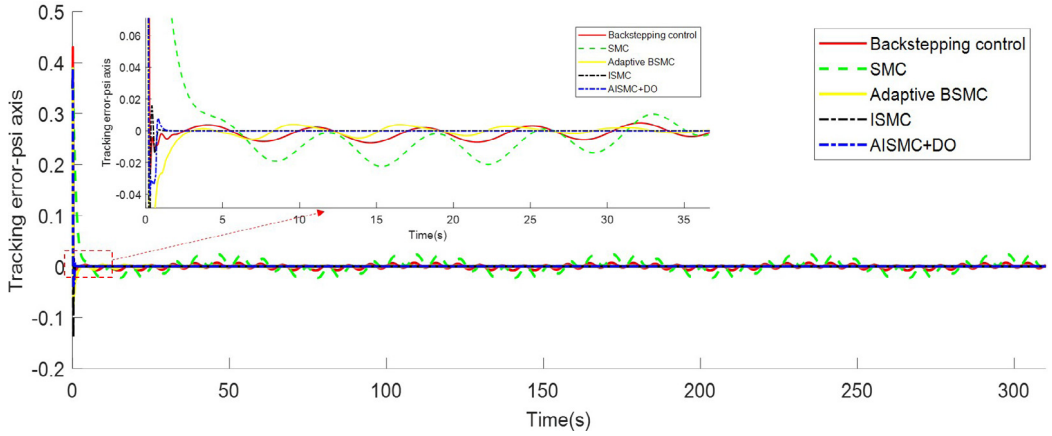


**Fig. 5.** Comparison in tracking error in $\psi$-axis among the Backstepping control, SMC, Adaptive BSMC, ISMC, and AISMC+DO.

for $(xy)$-axis and $\psi$-axis, respectively, and the AISMC+DO provides 0.0012 and $2.5653 \times 10^{-4}$ for $(xy)$-axis and $\psi$-axis, respectively.

The performance of the disturbance estimation of the AISMC+DO controller used in this paper is shown in Fig. 6. From Fig. 6, we can see that the developed DO provides very accurate disturbance estimation. In addition, in order to further verify the performance of the proposed DO, we compare it with the conventional DO [32–34]. The comparison in disturbance estimation error between the conventional DO and the proposed DO is shown in Fig. 7. It can be seen from Fig. 7 that the proposed DO provides lower estimation errors than the conventional one. In addition, an interesting point can be picked out from the Fig. 7 is that when the frequency of the disturbance is higher, the difference in estimation error between the conventional DO and the proposed DO is bigger; for example, the difference in $\psi$-axis is bigger than that of in $x$-axis and in $y$-axis. This is because, according to (41), the estimation error of the conventional DO is proportional to the derivative of the disturbance (when the frequency of the disturbance is high, the derivative will be high). In contrast, according to (38), the effects of the derivative of disturbance has been compensated properly in the design of proposed DO. Since the system obtains high accuracy of disturbance estimation, the sliding gain of the AISMC+DO can be selected as a smaller value compared to the ISMC. The convergences of the adaptation gains of the AISMC+DO are illustrated in Fig. 8. From Fig. 8, it can be observed that the adaptation gains converge to the stable values very quick (less than one second). Interestingly, although the AISMC+DO used smaller sliding gains (approximate 14.1, 16 and 16.5 (shown in Fig. 8)) than the ISMC (the sliding gains of the ISMC are 100, 100 and 100 (selected as in Table 1)), which lead to smaller chattering, the tracking performance of the AISMC+DO is comparable to the ISMC, as shown in Table 3. Therefore, theoretically, if we consider both the tracking error and chattering elimination, the AISMC+DO provides better tracking performance than the ISMC. Therefore, we can conclude that the proposed AISMC+DO is the best among compared controllers in this simulation study. The control efforts of the controllers are shown in Fig. 9. From Fig. 9, we can see that the control efforts are smooth and reasonable.

**Table 3**
Comparison between the controllers in terms of root mean square error (RMSE).

| RMSE controller | $\|E_{xy}\|$ | $\|E_{\psi}\|$ |
|---|---|---|
| Backstepping control | 0.0067 | 0.0136 |
| SMC | 0.0050 | 0.0147 |
| Adaptive BSMC | 0.0020 | 0.0021 |
| ISMC | 0.0013 | $2.3915 \times 10^{-4}$ |
| AISMC+DO | 0.0012 | $2.5653 \times 10^{-4}$ |

## 6. Conclusions

A new approach based on a composite adaptive integral sliding mode control and disturbance observer has been developed for tracking control of fully actuated surface vessels. First, an integral sliding mode control scheme has been reconstructed properly such that the reaching phase could be eliminated. The backstepping control technique has been employed for designing of nominal controller to ensure the stability of the system. Then, in order

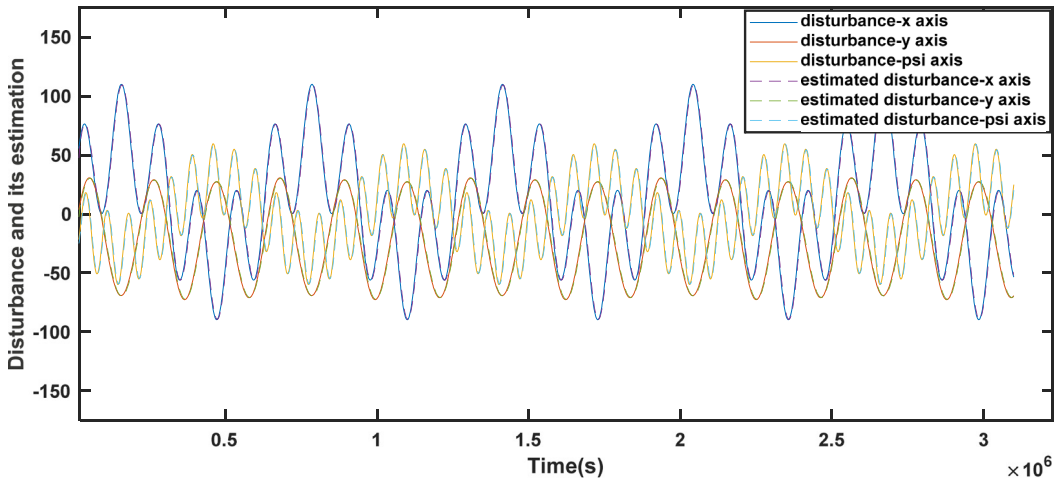


**Fig. 6.** Real disturbance and estimated disturbance observer of the proposed disturbance observer.

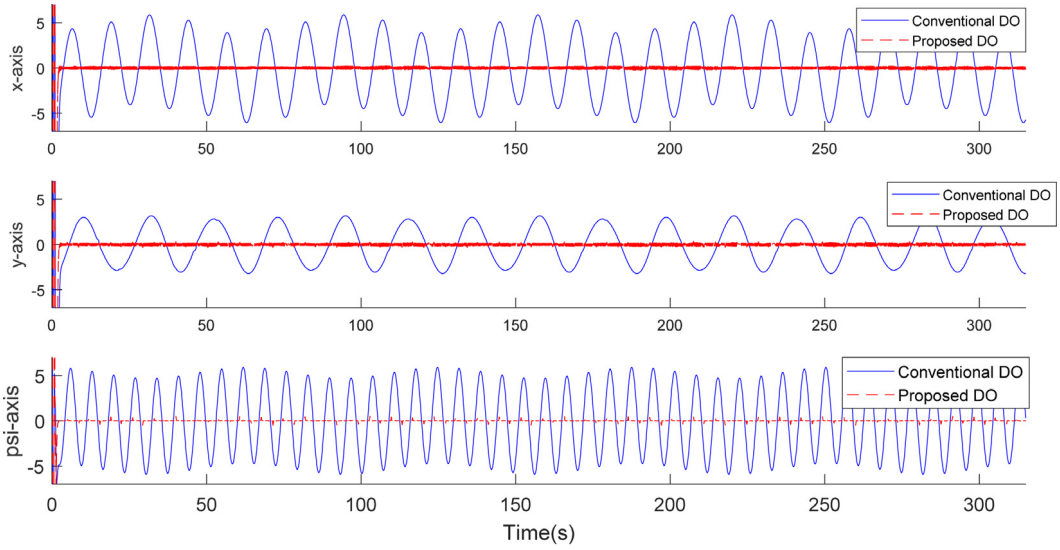


**Fig. 7.** Comparison in disturbance estimation error between the conventional disturbance observer and the proposed disturbance observer.

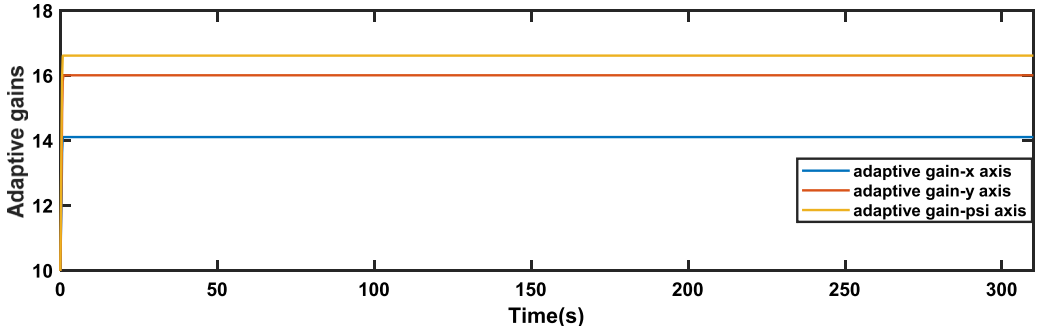


**Fig. 8.** Convergence of the adaptive gains of the AISMC+DO.

to reduce the chattering, an adaptive control law and a new disturbance observer have also been developed. The stability of the nominal controller and the whole integral sliding mode control scheme has been proven based on Lyapunov criteria. The proposed approaches have been compared with other state-of-the-art control techniques such as CBC, SMC and adaptive BSMC. The comparison results verified the superior performance of the proposed controller.

In this paper, the constraints on the control inputs and state outputs, which may be required in practical applications, have not been considered yet. The effectiveness of the proposed method for constraints system will be studied in the future works.

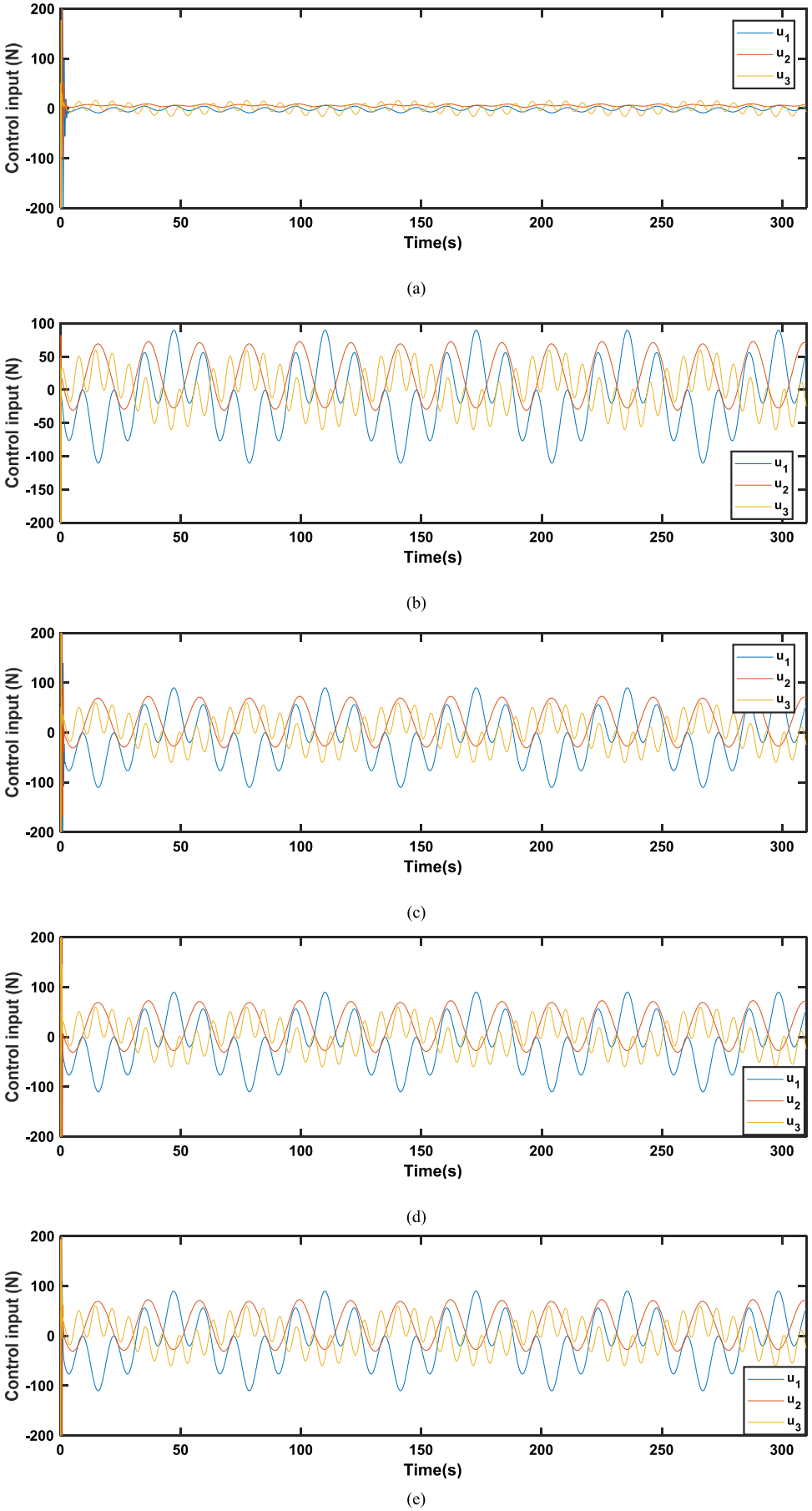


**Fig. 9.** Control efforts of the controllers. (a) Backstepping control, (b) SMC, (c) Adaptive BSMC, (d) ISMC and (e) AISMC+DO.

## Conflict of interests

The authors declare that they have no known competing financial interests or personal relationships that could have appeared to influence the work reported in this paper.

## Appendix A

**Theorem 2** (*Lyapunov Stability: [37]*). *Let* $\dot{z} = f(z)$ *and* $f(0) = 0$ *where* $z = 0$ *is in the interior of* $\Omega \subset \Re^n$. *Assume that* $V: \Omega \to \Re$ *is a* $C^1$ *function. If*

*(i)* $V(0) = 0$
*(ii)* $V(z) > 0$, *for all* $x \in \Omega, x \neq 0$
*(iii)* $\dot{V}(z) < 0$ *for all* $z \neq 0, \dot{V}(0) = 0$

*Then, every trajectory of the system* $\dot{z} = f(z)$ *converges to zero as* $t \to \infty$*(i.e., the system is globally asymptotically stable.*

## Appendix B

The sliding mode control (SMC) for the tracking control of a surface vessel can be described as follows:

Sliding surface is selected as:

$$s = \dot{e} + \lambda e \tag{61}$$

where $e = \eta - \eta_d$. The derivative of the sliding surface is

$$\dot{s} = \ddot{e} + \lambda\dot{e} = \Lambda u + \Gamma(\upsilon, \eta) + \Delta(\eta, \upsilon) - \dot{x}_{2d} + \lambda\dot{e} \tag{62}$$

Based on (62), the SMC is designed as

$$u(t) = \Lambda^{-1}\left(u_n(t) - u_s(t)\right) \tag{63}$$

where, the equivalent control input is designed as

$$u_n(t) = -\Gamma(\upsilon, \eta) + \dot{x}_{2d} - \lambda\dot{e} \tag{64}$$

and

$$u_s(t) = (\rho + \varpi)sign(s) \tag{65}$$

In order to alleviate the chattering phenomenon due to the used $sign(s)$ function. The continuous function below is used instead:

$$u_s(t) = (\rho + \varpi)\frac{s}{|s| + c} \tag{66}$$

where $c \in \Re$ is a small positive scalar.

## References


[1] Xiao B, Yang X, Huo X. A novel disturbance estimation scheme for formation control of ocean surface vessels. IEEE Trans Ind Electron 2017;64(6):4994–5003.
[2] Dai SL, Wang M, Wang C. Neural learning control of marine surface vessels with guaranteed transient tracking performance. IEEE Trans Ind Electron 2016;63(3):1717–27.
[3] Zhao Z, He W, Ge SS. Adaptive neural network control of a fully actuated marine surface vessel with multiple output constraints. IEEE Trans Control Syst Technol 2014;22(4):1536–43.
[4] He W, Yin Z, Sun C. Adaptive neural network control of a marine vessel with constraints using the asymmetric barrier lyapunov function. IEEE Trans Cybern 2017;47(7):1641–51.
[5] Holzhüter T. LQG approach for the high-precision track control of ships. IEE Proc Control Theory Appl 1997;144:121–7.
[6] Fang MC, Lin YH, Wang BJ. Applying the PD controller on the roll reduction and track keeping for the ship advancing in waves. Ocean Eng 2012;54:13–25.
[7] Källström CG. Autopilot and track-keeping algorithms for high-speed craft. Control Eng Pract 2000;8(2):185–90.
[8] Fang MC, Zhuo YZ, Lee ZY. The application of the self-tuning neural network PID controller on the ship roll reduction in random waves. Ocean Eng 2010;37(7):529–38.
[9] Ghommam J, Mnif F, Benali A, Derbel N. Asymptotic backstepping stabilization of an underactuated surface vessel. IEEE Trans Control Syst Technol 2006;14(6):1150–7.
[10] Park BS, Kwon JW, Kim H. Neural network-based output feedback control for reference tracking of underactuated surface vessels. Automatica 2017;77:353–9.
[11] Zhao Z, He W, Ge SS. Adaptive neural network control of a fully actuated marine surface vessel with multiple output constraints. IEEE Trans Control Syst Technol 2014;22(4):1536–43.
[12] He W, Yin Z, Sun C. Adaptive neural network control of a marine vessel with constraints using the asymmetric barrier lyapunov function. IEEE Trans Cybern 2017;47(7):641–1651.
[13] Dai SL, Wang M, Wang C. Neural learning control of marine surface vessels with guaranteed transient tracking performance. IEEE Trans Ind Electron 2016;63(3):1717–27.
[14] Velagic J, Vukic Z, Omerdic E. Adaptive fuzzy ship autopilot for track-keeping. Control Eng Pract 2013;11(4):433–43.
[15] Lee TH, Cao Y, Lin YM. Dynamic positioning of drilling vessels with a fuzzy logic controller. Int J Syst Sci 2010;33(12):979–93.
[16] Wang N, Er MJ. Direct adaptive fuzzy tracking control of marine vehicles with fully unknown parametric dynamics and uncertainties. IEEE Trans Control Syst Technol 2016;24(5):1845–52.
[17] Tee KP, Ge SS. Control of fully actuated ocean surface vessels using a class of feedforward approximators. IEEE Trans Control Syst Technol 2006;14(4):750–6.
[18] Yan Z, Wang J. Model predictive control for tracking of underactuated vessels based on recurrent neural networks. IEEE J Ocean Eng 2012;37(4):717–26.
[19] Li Z, Sun J. Disturbance compensating model predictive control with application to ship heading control. IEEE Trans Control Syst Technol 2012;20(1):257–65.
[20] Abdelaal M, Fränzle M, Hahn A. Nonlinear model predictive control for trajectory tracking and collision avoidance of underactuated vessels with disturbances. Ocean Eng 2018;160:168–80.
[21] Utkin V. Sliding modes on control and optimization. Berlin, Germany: Springer-Verlag; 1992.
[22] Ashrafiuon H, Muske KR, McNinch LC, Soltan RA. Sliding-mode tracking control of surface vessels. IEEE Trans Ind Electron 2008;55(11):4004–12.
[23] Yu R, Zhu Q, Xia G, Liu Z. Sliding mode tracking control of an underactuated surface vessel. IET Control Theory Appl 2012;6(3):461–6.
[24] Fahimi F. Sliding-mode formation control for underactuated surface vessels. IEEE Trans Robot 2017;23(3):617–22.
[25] Yin S, Xiao B. Tracking control of surface ships with disturbance and uncertainties rejection capability. IEEE/ASME Trans Mech 2017;22(3):1154–62.
[26] Hamayun MT, Edwards C, Alwi H. Design and analysis of an integral sliding mode fault-tolerant control scheme. IEEE Trans Automat Control 2012;57(7):1783–9.
[27] Van M. Adaptive neural integral sliding mode control for tracking control of fully actuated uncertain surface vessels. Int J Robust Nonlinear Control. 2019;1–21.
[28] Cao WJ, Xu JX. Nonlinear integral-type sliding surface for both matched and unmatched uncertain systems. IEEE Trans Auto Cont 2004;49(8):1355–60.
[29] Xu JX, Guo ZQ, Lee TH. Design and implementation of integral sliding-mode control on an underactuated two-wheeled mobile robot. IEEE Trans Ind Electron 2014;61(7):3671–81.
[30] Qin J, Ma Q, Gao H, Zheng WX. Fault-tolerant cooperative tracking control via integral sliding mode control technique. IEEE/ASME Trans Mech 2018;23(1):342–51.
[31] Xiao B, Yang X, Huo X. A novel disturbance estimation scheme for formation control of ocean surface vessels. IEEE Trans Ind Electron 2017;64(6):4994–5003.
[32] He W, Yan Z, Sun C, Chen Y. Adaptive neural network control of a flapping wing micro aerial vehicle with disturbance observer. IEEE Trans Cybern 2017;47(10):3452–65.
[33] Du J, Hu X, Kristic M, Sun Y. Robust dynamic positioning of ships with disturbances under input saturation. Automatica 2016;73:207–14.
[34] Chen WH, Yang J, Guo L, Li S. Disturbance-observer-based control and related methods—an overview. IEEE Trans Ind Electron 2016;63(2):1083–95.
[35] Cao Y, Chen XB. Disturbance-observer-based sliding-mode control for a 3-DOF nanopositioning stage. IEEE/ASME Trans Mech 2014;19(3):924–31.
[36] Liu J, Gao Y, Su X, Wack M, Wu L. Disturbance-observer-based control for air management of PEM fuel cell systems via sliding mode technique. IEEE Trans Control Syst Technol 2018. http://dx.doi.org/10.1109/TCST.2018.2802467.
[37] Khalil HK. Nonlinear systems (3rd ed.). Upper Saddle River, NJ: Prentice Hall.
[38] Levant A. Robust exact differentiation via sliding mode technique. Automatica 1998;34(3):379–84.
[39] Van M, Ge SS, Ren H. Finite time fault tolerant control for robot manipulators using time delay estimation and continuous nonsingular fast terminal sliding mode control. IEEE Trans Cybern 2017;47(7):1681–93.
[40] Van M, Ge SS, Ren H. Robust fault tolerant control for a class second-order nonlinear systems using an adaptive third-order sliding mode control. IEEE Trans Syst Man Cybern Syst 2017;47(2):221–8.